The AAPS Journal 2004; 6 (3) Article 23 (http://www.aapsj.org).

Etoposide-incorporated Tripalmitin Nanoparticles With Different Surface Charge: Formulation, Characterization, Radiolabeling, and Biodistribution Studies

Submitted: March 8, 2004; Accepted: July 10, 2004; Published: October 7, 2004.

Lakkireddy Harivardhan Reddy,[1] Rakesh Kumar Sharma,[2] Krishna Chuttani,[2] Anil Kumar Mishra,[2] and Rayasa Ramachandra Murthy[1]

[1]Drug Delivery Research Laboratory, Center of Relevance and Excellence in NDDS, Pharmacy Department, G. H. Patel Building, Donor's Plaza, Fatehgunj, M. S. University, Baroda-390002, Gujarat, India
[2]Department of Radiopharmaceuticals and Radiation Biology, Institute of Nuclear Medicine and Allied Sciences, Brigadier S. K. Mazumdar Road, Delhi-110054, India

ABSTRACT

Etoposide-incorporated tripalmitin nanoparticles with negative (ETN) and positive charge (ETP) were prepared by melt emulsification and high-pressure homogenization techniques. Spray drying of nanoparticles led to free flowing powder with excellent redispersibility. The nanoparticles were characterized by size analysis, zeta potential measurements, and scanning electron microscopy. The mean diameter of ETN and ETP nanoparticles was 391 nm and 362 nm, respectively, and the entrapment efficiency was more than 96%. Radiolabeling of etoposide and nanoparticles was performed with Technetium-99m (^{99m}Tc) with high labeling efficiency and in vitro stability. The determination of binding affinity of ^{99m}Tc-labeled complexes by diethylene triamine penta acetic acid (DTPA) and cysteine challenge test confirmed low transchelation of ^{99m}Tc-labeled complexes and high in vitro stability. Pharmacokinetic data of radiolabeled etoposide, ETN, and ETP nanoparticles in rats reveal that positively charged nanoparticles had high blood concentrations and prolonged blood residence time. Biodistribution studies of ^{99m}Tc-labeled complexes were performed after intravenous administration in mice. Both ETN and ETP nanoparticles showed significantly lower uptake by organs of the reticuloendothelial system such as liver and spleen ($P < .001$) compared with etoposide. The ETP nanoparticles showed a relatively high distribution to bone and brain (14-fold higher than etoposide and ETN at 4 hours postinjection) than ETN nanoparticles. The ETP nanoparticles with long circulating property could be a beneficial delivery system for targeting to tumors by Enhanced Permeability and Retention effect and to brain.

KEYWORDS: etoposide, tripalmitin, Technetium-99m, long circulating nanoparticles, radiolabeling, biodistribution.

Corresponding Author: Rayasa Ramachandra Murthy, Drug Delivery Research Laboratory, Center of Relevance and Excellence in NDDS, Pharmacy Department, G. H. Patel Building, Donor's Plaza, Fatehgunj, Baroda-390002, Gujarat, India. Tel: +91-265-2794051. Fax: +91-265-2423898. Email: m_rsr@rediffmail.com.

INTRODUCTION

Lipid nanoparticles are an alternative drug delivery system to emulsions, liposomes, and polymeric nanoparticles.[1] The inherent property of the solid nature of lipids and the ability to form smaller particles as well as their stability has popularized their use in drug delivery.[1] Lipid nanoparticles are usually aqueous dispersions of solid lipids or dry powders obtained by lyophilization[2] or spray drying.[3] Lipid nanoparticles overcome the membrane stability and drug-leaching problems associated with liposomes and emulsions,[4] and the biodegradation and toxicity problems of polymeric nanoparticles,[5] and facilitate prolonged drug release.[6] Lipid nanoparticles are prepared from biocompatible lipids and possess excellent biodegradability and low toxicity.[5,7]

Lipid nanoparticles have received great attention as drug carriers in recent years. A striking advantage of lipid nanoparticles is the feasibility of large-scale production by a high-pressure homogenization technique.[8] Several reports are available on formulation, characterization,[8,9] sterilization,[10] in vitro degradation, and lipid recrystallization behavioral studies by various techniques[11] (eg, differential scanning calorimetry [DSC],[12] small-angle and wide-angle x-ray diffractometry[13]) and on their in vitro drug release potential.[12] Extensive work by Bunjes and coworkers[14-16] reports on crystalline properties of lipids and their recrystallization patterns during nanoparticle preparation, and the influence of nanoparticle size on recrystallization pattern. Recent reviews by Mehnert and Mader[17] and by Muller and coworkers[18] provide extensive information on nanoparticle preparation, characterization, and drug release properties.

To date, the majority of studies reported the application of lipid nanoparticles for peroral administration for the improvement of bioavailability of poorly soluble drugs.[19,20] Of interest is that despite the advantages of lipid nanoparticles with respect to their ease of preparation, stability, and drug incorporation and release potential, only a few studies are available on their use in parenteral drug delivery and their fate in vivo.[21] Attempts to modify the surface characteristics of lipid nanoparticles, apart from the hydrophilic coatings to modify their in vivo fate, are

largely neglected. The surface properties of particulate carriers greatly define their in vivo fate. The extent and nature of opsonin adsorption at the surface of colloidal particles and their simultaneous blood clearance depend on the physicochemical properties of the particles, such as size, surface charge, and surface hydrophobicity.[22] The charge carried by the colloidal particles can have an important role in determining the clearance and fate of the particles.[22] Recently, several reports appeared on incorporation of polyethylene glycol (PEG) moieties for prolonged blood circulation,[23] and on the use of charged lipids to modify the biodistribution of liposomes.[24] Our recent report on cyclosporine-loaded charged liposomes revealed that the surface charge greatly influenced their biodistribution pattern.[25] Keeping in view the inherent advantages of lipid nanoparticles, attempts were made to formulate nanoparticles with charged lipids and evaluate their blood profile and biodistribution pattern.

Etoposide is an anticancer agent that is used in the treatment of a variety of malignancies, such as malignant gliomas, and has been demonstrated to be effective in the treatment of small cell lung cancer (SCLC), malignant lymphoma, and ovarian cancer. It acts by inhibition of topoisomerase II and activation of oxidation reduction reactions to produce derivatives that bind directly to DNA and cause DNA damage.[26,27]

We are working on a program on radiolabeling of drugs and particulate systems to study their organ distribution pattern and fate in vivo. Our recent reports showed success in the formation of stable radiolabeled complexes of drugs and liposomes.[25,28,29] We hereby report our experience to formulate etoposide-incorporated, negatively charged tripalmitin nanoparticles (ETN) and positively charged tripalmitin nanoparticles (ETP) using stearyl amine by melt emulsification and high-pressure homogenization, and their characterization by particle size analysis, zeta potential measurements, and scanning electron microscopy (SEM). The drug and nanoparticles were radiolabeled with ^{99m}Tc and their in vitro stability was evaluated. The radiolabeled complexes were intravenously administered and the studies of blood clearance were performed in rats and biodistribution in mice.

Materials and Methods

Chemicals

Etoposide was a kind gift from Dabur Research Center (Ghaziabad, India) and Cipla Limited (Mumbai, India). Tripalmitin was purchased from Sisco Laboratories (Mumbai, India). Hydrogenated soya phosphatidyl choline (HSPC) was purchased from Lipoid Gmbh (Ludwigshafen, Germany). Diethylene triamine penta acetic acid (DTPA) and cysteine were purchased from Sigma Chemical Co (St Louis, MO). Sodium pertechnetate prepared from molybdenum-99 by solvent extraction was procured from the Regional Center for Radiopharmaceutical Dispensing (Northern Region), Board of Radiation and Isotope Technology (BRIT) (Delhi, India). Sodium tauroglycocholate and stannous chloride were purchased from Qualigens (Mumbai, India). All other chemicals used in the study were of analytical grade.

Preparation of Tripalmitin Nanoparticles

Tripalmitin nanoparticles were prepared by melt emulsification and homogenization technique. Etoposide was dissolved in a small quantity of methanol (0.2 mL), to it was added HSPC, and the mixture was warmed slightly to form a clear melt. The methanol was then evaporated completely by heating the phase to between 50°C and 55°C. This drug containing HSPC was added to tripalmitin and heated to obtain a clear melt. The melt was then heated to 5°C above the melting point of tripalmitin and emulsified using a blade-type stirrer (Remi, Mumbai, India) at 2000 rpm into the aqueous phase containing 3% wt/vol sodium tauroglycocholate, which was preheated to 5°C above the temperature of the lipid phase. The hot emulsion was then homogenized at a pressure of 10 000 psi for 3 cycles in the high-pressure homogenizer (Avestin, Ottawa, ON, Canada) maintained in a water bath at 90°C. The nanodispersion formed was spray dried using a spray drier (JISL Instruments, Mumbai, India) after the addition of 2 parts by weight lactose monohydrate with respect to the total lipid content in the formulation. Spray drying was performed only for ETN nanoparticles; the nanodispersion of ETP nanoparticles was used for the further studies.

ETP nanoparticles were prepared by incorporating 10 mol% stearyl amine (positively charged lipid), with respect to HSPC, into the mixture of tripalmitin and HSPC. The lipid melt was emulsified into hot aqueous solution of 3% wt/vol Poloxamer-407 and homogenized at a pressure of 10 000 psi for 3 cycles.

Drug Content Determination in Nanoparticles

The nanoparticles in dispersion were aggregated by adding 0.1 mL of 10 mg/mL protamine sulfate solution, and the dispersion was centrifuged to obtain the pellet. The supernatant was decanted and the pellet was washed with distilled water and lyophilized after the addition of 2 parts by weight sucrose with respect to total lipid content of the formulation. Twenty-five milligrams of lyophilized powder was dissolved in a mixture of methanol-chloroform (1:1); required dilutions were performed with the same solvent mixture and analyzed in a UV-visible spectrophotometer (Shimadzu, Japan) 286 nm.

Characterization of Tripalmitin Nanoparticles

Particle Size Analysis

The size analysis of nanoparticles was performed by laser diffraction using a Malvern Hydro 2000SM particle size ana-

lyzer (Malvern Instruments, Worcestershire, UK). The spray-dried powder was dispersed in distilled water (filtered through 0.22-µm membrane filter, Pall filters, Mumbai, India) and vortexed for 10 seconds. The nanoparticulate dispersion obtained was added to the sample dispersion unit containing stirrer and stirred in order to minimize the interparticle interactions; the laser obscuration range was maintained between 10% and 20%. The instrument was set to measure the sample 3 times at a rate of 3000 snaps (or counts) per second. The sample was counted 3 times and average volume mean diameter was obtained.

Zeta Potential Measurement

Zeta potential of ETN and ETP nanoparticles was measured in a Malvern Zetasizer 3000 HS_A (Malvern Instruments). The nanoparticles were dispersed in 7.4 pH phosphate-buffered saline, and the zeta potential was determined.

Scanning Electron Microscopy

The powder nanoparticles were stuck to a brass stub with double-sided adhesive tape. The stub was fixed into a sample holder and placed in the vacuum chamber of a Jeol JSM 1560 LV SEM (Jeol, Peabody, MA) and observed under low vacuum (10^{-3} torr).

Radiolabeling of Etoposide and Tripalmitin Nanoparticles

Etoposide, ETN, and ETP nanoparticles were labeled with Technetium-99m (^{99m}Tc) by reduction with stannous chloride using a method similar to that previously reported.[25,30] In brief, ^{99m}Tc (2 mCi) was reduced with stannous chloride (20 µg for etoposide and 60 µg for ETN and ETP nanoparticles) and pH was adjusted to 6.5 with 0.5 M sodium bicarbonate. To ^{99m}Tc was added etoposide (2 mg/mL), or ETN or ETP nanoparticles (equivalent to 2 mg/mL etoposide), and the mixture was incubated at room temperature for 10 minutes. Quality control was performed as per the method reported earlier.[31] The labeling efficiency of etoposide, ETN, and ETP nanoparticles was determined by ascending thin layer chromatography (TLC) using silica gel-coated fiber sheets (Gelman Sciences Inc, Ann Arbor, MI). The instant thin layer chromatography (ITLC) strip was spotted with 2 to 3 mL of the labeled complex at 1 cm up from the bottom and developed using acetone as the mobile phase. The solvent front was allowed to reach up to a height of ~8 cm from the origin. The strip was cut into 2 halves, and the radioactivity in each half was determined by a well-type gamma ray spectrometer (type GRS23C, Electronics Corporation of India Ltd, Hyderabad, India). The free pertechnetate (R_f = 0.9-1.0) migrates to the top portion of the ITLC strip, leaving the reduced/hydrolyzed ^{99m}Tc along with the labeled complex at the bottom. Incorporation of excess of stannous chloride for reduction of ^{99m}Tc may lead to the formation of radio colloids, which is undesirable. The colloid formation was determined in pyridine:acetic acid:water (3:5:1.5). The radio colloids remained at the bottom of the strip, while both the free pertechnetate and the labeled complex migrated with the solvent front. By subtracting the migrated activity with the solvent front using acetone from that using pyridine:acetic acid:water mixture, the net amount of ^{99m}Tc-etopsoide, ^{99m}Tc-ETN, and ^{99m}Tc-ETP nanoparticles was calculated.

Stability of the ^{99m}Tc-labeled Complexes

Stability of the ^{99m}Tc-labeled complexes of etoposide and tripalmitin nanoparticles was determined in vitro in human serum by ascending TLC technique. The labeled complex (0.1 mL) was incubated with freshly collected human serum (0.4 mL) at 37°C. The samples were withdrawn at regular intervals up to 24 hours and analyzed in gamma ray spectrometer.

DTPA and Cysteine Challenge

These studies were performed in order to check the strength of binding of ^{99m}Tc with the compounds. The studies were performed as previously reported.[32] In brief, fresh solutions of DTPA and cysteine (10, 30, and 50 mM) were prepared in 0.9% saline. Five hundred microliters of the labeled preparation was treated with different concentrations of DTPA and cysteine separately and incubated for 1 hour at 37°C. Five hundred microliters of 0.9% saline served as control. The effect of DTPA and cysteine on the labeling efficiency of complexes was measured by ITLC-silica gel strips using acetone as mobile phase. In this system ^{99m}Tc-etoposide, ^{99m}Tc-ETN, and ^{99m}Tc-ETP nanoparticle complexes remain at the origin (R_f = 0.0), while pertechnetate (R_f = 0.9-1.0) and all known chemical forms of ^{99m}Tc-DTPA and ^{99m}Tc-cysteine complexes migrate (R_f = 0.7-1.0). After developing, each paper was cut into 2 halves and each half was counted for radioactivity in gamma ray spectrometer.

Blood Clearance of Etoposide and Tripalmitin Nanoparticles in Rats

Sprague-Dawley rats of either sex weighing 250 to 300 g were selected for the blood clearance studies. Into the tail vein of rats, 0.2 mL of the ^{99m}Tc-labeled complexes of etoposide or ETN or ETP nanoparticles containing 200 µCi of ^{99m}Tc was intravenously injected. The blood samples were collected at 1 minute, 5 minutes, 15 minutes, 0.5 hour, 1 hour, 1.5 hours, 2 hours, 3 hours, 4 hours, 6 hours, and 24 hours from the retro-orbital plexus of rat eye and analyzed for the radioactivity in gamma ray spectrometer. The blood was weighed, and radioactivity in whole blood was calculated by considering the volume of blood as 7.3% of the total body weight.

Table 1. Influence of Homogenization Pressure and Number of Homogenization Cycles on the Mean Diameter of ETN Nanoparticles*

Homogenization Pressure (psi)	No. of Homogenization Cycles	Mean Particle Diameter (nm)	Particle Size, Width d (0.1) to d (0.9)
5000	1	1120.0 ± 21 nm	920-2224
5000	2	958.0 ± 17 nm	543-1700
5000	3	826.0 ± 13 nm	560-1520
5000	4	724.0 ± 15 nm	425-1450
10 000	1	574.0 ± 7 nm	509-663
10 000	2	414.0 ± 9 nm	295-628
10 000	3	358.0 ± 8 nm	313-425
10 000	4	356.0 ± 8 nm	281-525
15 000	1	597.0 ±12 nm	289-1185
15 000	2	375.0 ± 7 nm	296-470
15 000	3	361.0 ± 10 nm	296-470
15 000	4	421.0 ± 5 nm	307-511

*ETN indicates etoposide-loaded negatively charged tripalmitin nanoparticles; d (0.1) corresponds to the diameter of 10% of particles; and d (0.9) corresponds to the diameter of 90% of particles measured.

Table 2. Optimized Conditions for the Spray Drying of ETN*

Spray-drying Parameters	Optimized Conditions
Inlet air pressure	2.5 kg/cm^2
Aspirator volume	50 cu ft/min
Flow rate	2 mL/min
Inlet temperature	70°C
Outlet temperature	40°C

*ETN indicates etoposide-loaded negatively charged tripalmitin nanoparticles.

Biodistribution Study

^{99m}Tc-labeled complexes of etoposide, ETN, and ETP nanoparticles were intravenously injected into healthy Balb/c mice weighing ~25 to 30 g. The biodistribution studies of etoposide were performed after 0.5 hour, 1 hour, 4 hours, and 24 hours postinjection, while for ETN and ETP nanoparticles, the studies were performed at 1 hour, 4 hours, and 24 hours postinjection. At these time intervals, the blood was collected by cardiac puncture, the animals were humanely killed, and the organs were isolated. The organs were then weighed and measured for radioactivity in gamma ray spectrometer. The radioactivity was interpreted as percentage of injected dose per gram of organ/tissue. All the animal experiments were approved by the Social Justice and Empowerment Committee for the purpose of control and supervision of experiments on animals, New Delhi, India.

Statistical Analysis

Statistical comparisons of the experimental results were performed by 1-way analysis of variance (ANOVA) at an α level of 0.05 and 0.001. The difference in results between the 2 groups was compared by Tukey-Kramer multiple comparison test at the significance levels of $P < .05$ and $P < .001$, respectively.

RESULTS

Etoposide-loaded tripalmitin nanoparticles with negative and positive charge were prepared by melt emulsification and high-pressure homogenization technique. The average mean diameters of ETN and ETP nanoparticle dispersions after homogenization were 358 nm and 362 nm, respectively. The ETN and ETP nanoparticles could incorporate 4% etoposide with 96.14% and 97.05% entrapment efficiency, respectively. Homogenization pressure and number of homogenization cycles greatly influenced the mean diameter of nanoparticles (Table 1). The optimum homogenization conditions were found to be 10 000 psi for 3 cycles. Although the homogenization at 10 000 psi for 4 cycles resulted in a decrease of 2 nm mean diameter compared with that of 3 cycles, the latter was considered optimum because the reduction in particle size after that was not significant. The ETN nanodispersion obtained after homogenization was spray dried after the addition of 2 parts by weight lactose monohydrate (a disaccharide) with respect to the total lipid content (ie, tripalmitin and HSPC) to obtain dry powder nanoparticles. The technique yielded good powder particles with excellent redispersibility in aqueous media. The mean diameter of particles was found slightly increased after spray drying (358 nm before spray drying and 391 nm after spray drying). The width of the particle distribution after spray drying was 307 nm to 497 nm, which indicates that 90% of particles possess diameters below 497 nm with a mean diameter of 391 nm. The optimized spray-drying conditions are shown in Table 2. SEM confirms the spherical nature of nanoparticles (Figure 1). The results of zeta potential measurements reveal that the ETN nanoparticles exhibited negative zeta potential (–46.6 ± 1.7 mV) and ETP nanoparticles exhibited positive zeta potential (5 ± 0.4 mV).

Etoposide, ETN, and ETP nanoparticles were radiolabeled with ^{99m}Tc with high labeling efficiency. The pertechnetate existing in its heptavalent oxidation state was reduced to a lower

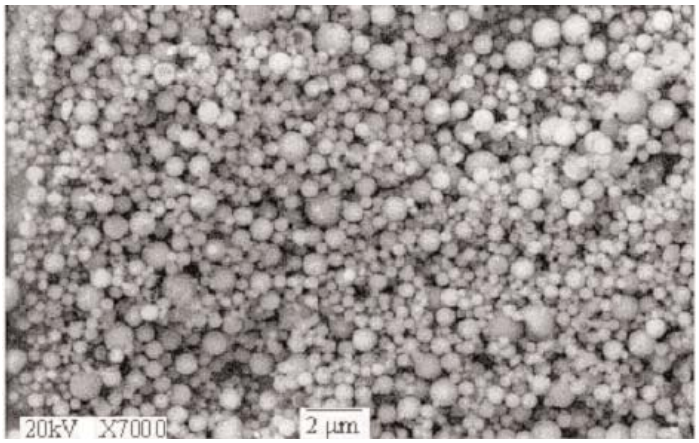

Figure 1. SEM of spray-dried ETN nanoparticles.

valence state by stannous chloride and the pH was adjusted to 6.5 before addition of etoposide or ETN or ETP nanoparticle dispersion. After conducting preliminary trials, the pH to be adjusted for the reduced ^{99m}Tc to obtain high labeling efficiency was optimized to 6.5. The amount of stannous chloride used for reducing the pertechnetate played an important role in the labeling process. The influence of the amount of stannous chloride on labeling efficiency and formation of radio colloids is shown in Tables 3 and 4. The optimum amount of stannous chloride resulting in high labeling efficiency and low amount of radiocolloids was found to be 20 µg for etoposide and 60 µg for the ETN and ETP nanoparticles. Lower amounts of stannous chloride led to poor labeling efficiency, and higher concentrations led to the greater formation of undesirable radiocolloids. The labeling efficiency and the stability of labeled complex were ascertained by ascending TLC.

In Vitro Stability of Labeled Complexes

DTPA and cysteine challenge studies were performed to obtain information on the transchelation (a measure of strength of binding). Challenge studies demonstrated that the labeling efficiency of the complexes did not alter much in the presence of DTPA (Figure 2) and cysteine (Figure 3). Even at 50 mM concentration of DTPA and cysteine, the transchelation was found to be less than 5%, indicating the stability of the radiolabeled complexes.

Table 3. Influence of the Amount of Stannous Chloride on the Labeling Efficiency of Etoposide*

	Etoposide		
$SnCl_2.2H_2O$ (µg)	% Labeled	% Colloids	% Free
5	80.24	0.45	19.31
10	88.76	0.48	1.76
20	99.28	0.68	0.04
25	98.25	1.18	0.57
50	96.78	3.01	0.21

*Each value is the mean of 3 experiments.

Serum Stability of Labeled Complexes

Table 5 represents the data of in vitro serum stability of ^{99m}Tc-labeled complexes of etoposide, ETN, and ETP nanoparticles determined up to 24 hours. The data demonstrated stability of the above radiolabeled complexes in serum. The serum stability of the labeled complexes indicates the usefulness of label as a marker for the biodistribution studies.

Blood Clearance Studies

Blood clearance studies of ^{99m}Tc-labeled complexes of etoposide, ETN, and ETP nanoparticles were investigated in healthy Sprague-Dawley rats. Both ETN and ETP nanoparticles exhibited higher blood concentrations compared with free etoposide (Figure 4). In particular, the ETP nanoparticles exhibited significantly higher concentration and extended residence time in blood compared with the ETN nanoparticles. The difference in blood concentrations of ETP and ETN was very high at 6 hours, but low at 24 hours postinjection. About 2.05% of the injected dose of ETP was recovered from blood even after 24 hours, indicating its long circulation capability. Such differential blood kinetics would also result in different biodistribution patterns.

Biodistribution Study

Table 6 represents the organ/tissue concentrations of intravenously injected ^{99m}Tc-etoposide nanoparticles and Table 7 represents the concentrations of ^{99m}Tc-ETN and ^{99m}Tc-ETP nanoparticles. Greater concentrations of free etoposide were found in the organs of the reticuloendothelial system (RES), such as liver, spleen, and lung. The overall uptake of ETN and

Table 4. Influence of the Amount of Stannous Chloride on the Labeling Efficiency of ETN and ETP*

	ETN			ETP		
$SnCl_2.2H_2O$ (µg)	% Labeled	% Colloids	% Free	% Labeled	% Colloids	% Free
10	85.74	0.25	14.01	87.56	0.19	12.25
30	92.26	0.38	7.36	93.45	0.29	6.26
60	98.85	0.68	0.47	98.32	0.56	1.12
75	94.48	3.85	1.67	95.85	3.21	0.94
100	92.85	7.01	0.14	93.26	6.12	0.62

*ETN indicates etoposide-loaded negatively charged tripalmitin nanoparticles; and ETP, etoposide-loaded positively charged tripalmitin nanoparticles. Each value is the mean of 3 experiments (n = 3).

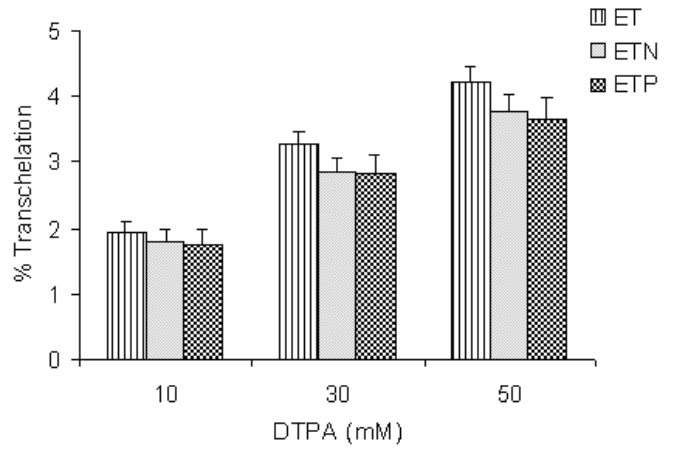

Figure 2. Effect of DTPA on transchelation of ^{99m}Tc-labeled complexes of etoposide (ET), ETN, and ETP nanoparticles. Each value is the mean of three experiments (n = 3).

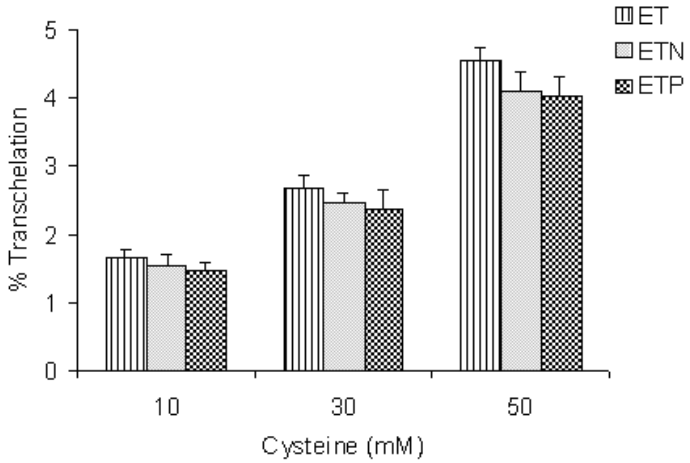

Figure 3. Effect of cysteine on transchelation of ^{99m}Tc-labeled complexes of etoposide (ET), ETN, and ETP nanoparticles. Each value is the mean of three experiments (n = 3).

ETP by liver and spleen was significantly lower than the free etoposide (< .001). The splenic uptake of both ETN and ETP was low initially (0.15% and 2.83% injected dose [ID] at 1 hour) but increased with time (0.72% and 3.76% ID at 4 hours). The uptake of free etoposide by lung tissues was high initially (9.91% ID at 1 hour) followed by a decrease later (7.4% ID at 4 hours). A reverse trend was observed for nanoparticle formulations, where both ETN and ETP showed increased uptake by lung with time (5.51% and 6.36% ID at 1 hour and 7.27% and 7.78% ID at 4 hours, respectively). No significant uptake of nanoparticles was found in the kidney, heart, and muscle. However, relatively high concentration of ETP was found in bone at 4 hours postinjection. The concentration of ETP nanoparticles was relatively higher in brain (10-fold and 14-fold higher than etoposide and ETN at 1 hour and 4 hours postinjection, respectively). Although the overall brain uptake of ETP nanoparticles was not very high, the significantly higher concentrations of ETP nanoparticles reaching the brain at 1 hour and 4 hours postinjection and even at 24 hours postinjection compared with etoposide and ETN

Table 5. Stability of ^{99m}Tc-labeled Complexes of Etoposide, ETN, and ETP Nanoparticles in Human Serum*

	% Radiolabeling		
Time (hours)	**Etoposide**	**ETN**	**ETP**
Initial	99.28	98.85	98.32
0.25	99.20	98.80	98.81
0.5	99.22	98.78	98.86
1	99.10	98.68	98.59
2	99.01	98.31	98.25
4	98.94	98.12	98.08
8	98.78	98.02	98.10
24	97.79	97.12	97.31

* ^{99m}Tc indicates Technetium-99m; ETN, etoposide-loaded negatively charged tripalmitin nanoparticles; and ETP, etoposide-loaded positively charged tripalmitin nanoparticles. Each value is the mean of 3 experiments (n = 3). The high labeling efficiency of complexes even at 24 hours indicates their serum stability.

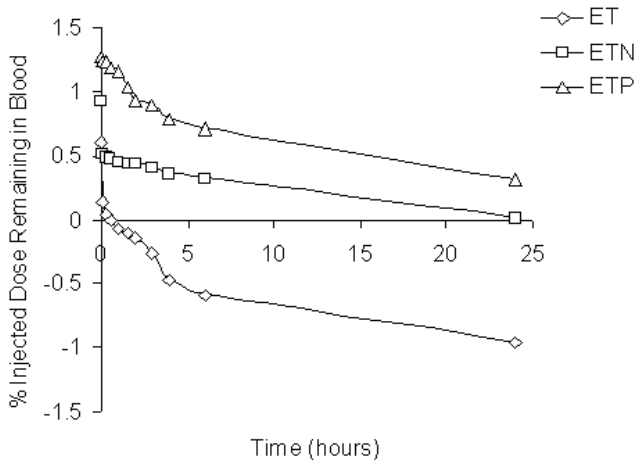

Figure 4. Semilogarithmic percentage injected dose of ^{99m}Tc-etoposide (ET), ^{99m}Tc-ETN, and ^{99m}Tc-ETP nanoparticles remaining in blood after intravenous injection in rats. Data points represent the mean values of 3 experiments (n = 3).

nanoparticles suggests greater brain transport. ETP nanoparticles showed comparatively higher concentrations in bone that increased with time (0.18% ID at 1 hour and 0.97% ID 4 hours postinjection). The distribution of ETP nanoparticles to muscle was significantly higher (P < .001) than ETN nanoparticles and free etoposide and showed an increase with time. A very low radioactivity was recovered from stomach and intestine and showed constancy with time indicating the in vivo stability of the radiolabeled complexes.

DISCUSSION

Formulation and Characterization of Tripalmitin Nanoparticles

ETN and ETP nanoparticles were prepared by the melt emulsification homogenization method, and the former was spray dried in the presence of lactose monohydrate to obtain pow-

Table 6. Biodistribution Studies of ^{99m}Tc-Etoposide in Balb/c Mice*

	Percentage Injected Dose per Gram of Organ/Tissue (± SEM)			
Organ /Tissue	**0.5 Hour**	**1 Hour**	**4 Hours**	**24 Hours**
Blood	0.91 ± 0.01	0.78 ± 0.01	0.58 ± 0.02	0.18 ± 0.01
Heart	0.18 ± 0.02	0.16 ± 0.01	0.13 ± 0.01	0.11 ± 0.01
Liver	5.61 ± 0.02	4.1 ± 0.06	3.65 ± 0.03	3.12 ± 0.04
Lung	10.44 ± 0.13	9.91 ± 0.17	7.4 ± 0.05	2.99 ± 0.04
Spleen	12.03 ± 0.15	11.05 ± 0.13	10.78 ± 0.15	8.83 ± 0.11
Kidney	3.77 ± 0.09	2.75 ± 0.06	1.35 ± 0.07	1.6 ± 0.05
Muscle	0.05 ± 0.01	0.06 ± 0.02	0.04 ± 0.01	0.08 ± 0.02
Bone	0.12 ± 0.04	0.14 ± 0.03	0.19 ± 0.03	0.68 ± 0.03
Stomach	0.27 ± 0.08	0.23 ± 0.06	0.49 ± 0.04	0.37 ± 0.04
Intestine	0.63 ± 0.06	0.54 ± 0.08	0.42 ± 0.06	0.09 ± 0.05
Brain	0.02 ± 0.02	0.01 ± 0.01	0.01 ± 0.01	0.01 ± 0.01

* ^{99m}Tc indicates Technetium-99m. The animals were intravenously administered with 100 μCi of the ^{99m}Tc-etoposide and were humanely killed at 0.5 hour, 1 hour, 4 hours, and 24 hours postinjection. Radioactivity was counted in each organ and expressed as percentage of injected dose per gram of organ/tissue. Each value is the mean (± SEM) of 3 mice.

Table 7. Biodistribution Studies of ^{99m}Tc-ETN and ^{99m}Tc-ETP Nanoparticles in Balb/c Mice*

	Percentage Injected Dose per Gram of Organ/Tissue (± SEM)					
	1 Hour		**4 Hours**		**24 Hours**	
Organ/Tissue	**ETN**	**ETP**	**ETN**	**ETP**	**ETN**	**ETP**
Blood	0.38 ± 0.01	5.80 ± 0.04†	0.34 ± 0.02	4.65 ± 0.03†	0.15 ± 0.01	2.42 ± 0.03†
Heart	0.03 ± 0.01	0.86 ± 0.02	0.03 ± 0.01	0.95 ± 0.03	0.01 ± 0.02	0.27 ± 0.02
Liver	1.58 ± 0.05†	1.48 ± 0.06†	1.37 ± 0.07†	1.16 ± 0.05†	2.21 ± 0.04†	0.88 ± 0.06†
Lung	5.51 ± 0.12†	6.36 ± 0.17†	7.27 ± 0.13	7.78 ± 0.21†	1.00 ± 0.09†	1.12 ± 0.24†
Spleen	0.15 ± 0.03†	2.83 ± 0.07†	0.72 ± 0.02†	3.76 ± 0.10†	1.78 ± 0.03†	1.08 ± 0.06†
Kidney	0.34 ± 0.15†	2.08 ± 0.06†	1.21 ± 0.11†	1.98 ± 0.04†	0.42 ± 0.05†	1.45 ± 0.03
Muscle	0.01 ± 0.01‡	0.24 ± 0.02†	0.02 ± 0.01	0.37 ± 0.02†	0.05 ± 0.01	0.18 ± 0.01†
Bone	0.05 ± 0.02	0.18 ± 0.01	0.09 ± 0.02	0.97 ± 0.04	0.41 ± 0.08	0.78 ± 0.01
Stomach	1.16 ± 0.03	0.13 ± 0.02	1.87 ± 0.01	0.17 ± 0.02	0.34 ± 0.03	0.20 ± 0.02
Intestine	0.15 ± 0.03	0.22 ± 0.06	0.50 ± 0.04	0.25 ± 0.03	0.12 ± 0.01	0.18 ± 0.02
Brain	0.01 ± 0.01	0.1 ± 0.01†	0.01 ± 0.01	0.14 ± 0.01†	0.02 ± 0.04	0.07 ± 0.02†

* ^{99m}Tc indicates Technetium-99m; ETN, etoposide-loaded negatively charged tripalmitin nanoparticles; and ETP, etoposide-loaded positively charged tripalmitin nanoparticles. The animals were intravenously administered with 100 μCi of the ^{99m}Tc-ETN and ^{99m}Tc-ETP nanoparticles and were humanely killed at 1 hour, 4 hours, and 24 hours postinjection. Radioactivity was counted in each organ and expressed as percentage of injected dose per gram of organ/tissue. Each value is the mean (± SEM) of 3 mice.

† indicates extremely significant ($P < .001$).

‡ indicates very significant ($P < .01$).

der nanoparticles. Sodium tauroglycocholate was used as surfactant for the formation of tripalmitin nanoparticles. The use of bile salts, such as sodium glycocholate, in the formation of nanoparticles with satisfactory long-term stability, has been reported.[33,34] The nanoparticles could incorporate 4% etoposide with 96.14% and 97.05% entrapment efficiency for ETN and ETP, respectively. According to the earlier report,[12] the crystallization of the melted triglycerides very often causes drug expulsion from the lipid resulting in low drug entrapment. But in our case, the nanoparticles showed maximum entrapment of etoposide. According to Westesen and coworkers,[12] the drug-loading capacity of the lipid carriers is limited owing to the generally low solubilization capacity of the molten lipids for many poorly water-soluble drugs, thus implying that entrapment efficiency is dependent on the solubility of drug in the lipid portion. In our case, the etoposide was poorly soluble in tripalmitin but was fairly soluble in HSPC in the quantities used in the formulation. Also in this case, the drug was particularly associated with the HSPC portion, and the expulsion of drug due to modified crystallization is unlikely. According to Bunjes and coworkers,[13] the crystallization habits of tripalmitin nanoparticles also vary with the quantity of drug incorporated. The above-described differences may be responsible for the observed higher entrapment efficiencies of ETN and ETP nanoparticles. However, we did not perform the recrystallization studies of these nanoparticles and may need further investigations to support the maximum entrapment efficiency of drug obtained in our case.

High-pressure homogenization was reported to be the most reliable technique for the preparation of lipid nanoparticles with smaller size.[17] Very high shear stress and cavitation forces produced during homogenization disrupt the particles down to submicron range.[17] Another advantage of this method is that it avoids the use of organic solvents. Homogenization of hot emulsion was performed at various homogenization pressures at different number of cycles, and mean particle diameter at each pressure and cycle number was recorded. Homogenization pressures above 10 000 psi did not show much improvement in mean particle diameter, while low pressures resulted in higher mean particle size. Homogenization at 10 000 psi for 3 cycles at 90°C water bath temperature resulted in nanoparticles of low mean diameter. Spray drying of nanodispersion did not result in significant increase in mean particle diameter. Controlled spray drying led to the yield of more than 75%. The high yield coupled with minimum increase in particle size indicates that the spray drying is an efficient method of obtaining powder nanoparticles. The mean diameter of the spray-dried nanoparticles, determined after reconstitution in distilled water, did not alter significantly (395nm) even after 3 months of preparation.

According to Westesen and Siekmann,[35] the lipids prefer to crystallize in the platelet form; hence the shape of nanoparticles very often differs from a spherical form. In contrast, the SEM of spray-dried ETN nanoparticles shows the spherical nature of the particles. The differences in the results may be attributed to the differences in composition used for the nanoparticle preparation. The ETN nanoparticles contain 6% wt/vol lipid content (of which 4.5% wt/vol is tripalmitin) stabilized by 3% wt/vol sodium tauroglycocholate (anionic surfactant). Increase in the lipid content in the formulation over 5% to 10% has been reported to cause the formation of particles with broader distribution and to include microparticles also.[36] Bunjes et al reported the differences in crystallization of tripalmitin when surfactants of different type and chain lengths were used.[14] These differences were attributed to the influence of head group and chain lengths of surfactants on the crystallization temperature of tripalmitin. The use of ionic surfactants along with phospholipids for stabilization of solid lipid nanoparticles (SLN) was reported to reduce or prevent the formation of macroscopic structures (gel structures) in the nanoparticle dispersion compared with the nanoparticles stabilized by phospholipid alone[35] as the surfactant; the soluble nature of ionic surfactants can rapidly reach the increased surface of particles during recrystallization and stabilize the particle surface. The high concentration of sodium tauroglycocholate and HSPC used in the formulation of ETN nanoparticles might be responsible for controlled crystallization of tripalmitin to form spherical particles. Incorporation of lactose for spray drying of nanoparticle dispersion may also be responsible for the formation of spherical nanoparticles due to their surface coverage by lactose.

Zeta Potential Measurements

The zeta potential measurements of nanoparticles indicate that ETP nanoparticles are positively charged, while ETN nanoparticles possess negative charge. From the zeta potential of tripalmitin nanoparticles stabilized with 3% wt/vol Poloxamer-407 (-5.6 ± 1.0 mV), it is evident that the stabilizer has an effect on particle surface charge, but the effect of stearyl amine is predominant in case of ETP nanoparticles in the creation of positive charge.

Radiolabeling and In Vitro Stability of Labeled Complexes

Studies with different amounts of stannous chloride were performed to optimize parameters for maximum radiolabeling efficiency. The amount of stannous chloride above the optimum concentration results in undesirable radiocolloid formation, and these radiocolloids distribute extensively to the organs of RES owing to their macrophage uptake. The stannous chloride below the optimum concentration leads to poor labeling efficiency because of the incomplete reduction of pertechnetate (TcO_4^-) from its heptavalent oxidation state. Hence, optimization of the amount of stannous chloride is an important parameter in the radiolabeling of a compound. The in vitro stability of nanoparticles was assessed by DTPA and cysteine challenge test. DTPA and cysteine possess greater affinity to ^{99m}Tc. Upon incubation with the labeled complexes, the DTPA and cysteine cause transchelation, resulting in decrease in labeling of the complexes. The lower degree of transchelation of ^{99m}Tc-labeled complexes of etoposide, ETN, and ETP nanoparticles indicates that both DTPA and cysteine could not chelate ^{99m}Tc from the above preparations, implying their high degree of stability.

Determination of stability of the labeled complexes in serum is an important parameter that ensures the intactness of the label in the presence of proteins and many other substances present in serum. The stability of labeled complexes in serum also supports their stability in biological environment upon administration into the body and their use in determining the blood clearance and biodistribution patterns.

Blood Clearance and Biodistribution Studies

ETN and ETP nanoparticles showed longer half-life than free etoposide in blood. In particular, the ETP nanoparticles showed significantly greater concentrations and extended residence time in blood compared with the ETN nanoparticles all throughout the study. Etoposide showed rapid blood clearance with only 0.85% of the ID at 1 hour postinjection. The results are in agreement with our earlier report[25] on long-circulating, positively charged liposomes and with other previous reports.[37-38] The blood concentration of ETP nanoparticles at 24 hours postinjection was ~18.6-fold and 1.64-fold higher than free etoposide and ETN nanoparticles, respec-

tively. About 2.05% of ID of ETP was recovered from blood even after 24 hours, indicating its long circulation capability. An earlier report by Levchenko and coworkers[39] indicated that positively charged liposomes (containing stearylamine) exhibit relatively long circulation in blood compared with negatively charged liposomes (containing phosphatidic acid or phosphatidyl serine), but less than the plain liposomes. Our results are in agreement with the above report, and at the same time the blood concentrations were significantly higher for ETP nanoparticles than for ETN nanoparticles. Sengupta and coworkers[40] reported significantly enhanced plasma half-life of etoposide incorporated into cationic liposomes prepared using stearylamine as positively charged lipid. Yu and Lin[41] also reported that the positively charged liposomes resulted in higher plasma-liposome concentration than the negatively charged liposomes. The positively charged liposomes are shown to be most stable in blood and to bind the lowest amount of protein,[42] which, in turn, is less prone to phagocytic uptake owing to the low opsonization. This finding clearly indicates the influence of positive charge on the enhancement of blood concentrations and circulation time of colloidal carriers. Hence, the greater blood concentrations and circulation time observed in the case of ETP nanoparticles are mainly the result of its positively charged surface. However, the contribution of Poloxamer-407 as steric stabilizer in ETP nanoparticles to such significant difference in the blood clearance cannot be ignored. Such a system with prolonged circulation may act as a circulating depot for drugs, improve the half-life, and infiltrate at greater concentrations into the leaky endothelial cells of tumor tissues by enhanced permeability and retention (EPR) effect.[43]

The uptake and distribution of ETN and ETP nanoparticles were found to be different to different organs. The rapid distribution of free etoposide to the organs of RES is owing to its affinity for those organs. From Figure 4 it is evident that the ETN nanoparticles exhibited relatively higher concentrations in blood compared with free etoposide. This finding might be the reason for the observed low concentrations of ETN in RES organs compared with free etoposide. The uptake of both types of nanoparticles by RES organs such as liver and spleen was significantly lower than the etoposide. On the other hand, ETP nanoparticles resulted in relatively higher muscle and bone concentrations than etoposide and ETN nanoparticles. The lower kidney concentrations of both types of nanoparticles indicate their slow excretion, and lower incidence of drug-associated kidney toxicity. Higher brain concentrations of ETP nanoparticles can be attributed to their preferential uptake by brain endothelial cells and suggest enhanced brain transport. The relatively high concentrations in muscle and bone are also owing to their extended residence time in blood. Although the brain concentration of ETP nanoparticles is not very high, the potential use of this system in the observed concentrations in the treatment of brain malignancies is considerable, as etoposide is also used in the treatment of brain malignancies such as brain stem gliomas.[26,27] The differences observed in the blood clearance and biodistribution studies with ETP nanoparticles can be mainly attributed to their positive charge and is partly due to the steric effect of Poloxamer-407. Very low stomach and intestine concentrations of the ^{99m}Tc-labeled complexes of etoposide as well as ETN and ETP suggest the intactness of the radiolabels with the preparations and their in vivo stability.

Conclusion

Etoposide-loaded tripalmitin nanoparticles with negative charge were developed as stable dry powder for reconstitution. The entrapment efficiency of both ETN and ETP nanoparticles was more than 96%. Radiolabeling of nanoparticles was performed with ^{99m}Tc, with high labeling efficiency and in vitro and in vivo stability. The pharmacokinetic data in rats showed higher blood concentrations and prolonged residence time of positively charged tripalmitin nanoparticles. The differences observed with the ETP nanoparticles in blood clearance and biodistribution are mainly owing to the positively charged surface and may be partly due to the steric stabilization property of Poloxamer-407 used as stabilizer. The relatively high brain concentration of ETP nanoparticles suggests their usefulness in the treatment of brain malignancies. The ETP nanoparticles of relatively smaller size coupled with prolonged blood circulating property could be a beneficial delivery system for tumor targeting of anticancer agents through EPR effect. Further investigations on the antitumor activity and tumor regression of ETP nanoparticles in lymphoma solid tumor are under progress in our laboratory.

Acknowledgements

Financial support from the University Grants Commission (F.10–32/2000 [SA-II]) New Delhi, India, is gratefully acknowledged. Leutinent General Turaga Ravindranath, Athivishishta Seva Medal (AVSM), Vishishta Seva Medal (VSM), director, Institute of Nuclear Medicine and Allied Sciences, Delhi, India, is acknowledged for providing necessary facilities to carry out the radiolabeling and biodistribution studies. The authors are also thankful to Dr Apte, University Department of Pharmaceutical Sciences, Kakatiya University, Warangal, India, for his help in carrying out the zeta potential measurements.

References

1. Muller RH, Olbrich C. Solid lipid nanoparticles: Phagocytic uptake, in vitro cytotoxicity and in vitro biodegradation. *Drugs Made Ger*. 1999;42:49-53.

2. Lim SJ, Kim CK. Formulation parameters determining the physicochemical characteristics of solid lipid nanoparticles loaded with all-trans retinoic acid. *Int J Pharm*. 2002;243:135-146.

3. Freitas C, Muller RH. Spray-drying of solid lipid nanoparticles (SLN™). *Eur J Pharm Biopharm*. 1998;46:145-151.

4. Magenheim B, Levy MY, Benita S. A new in vitro technique for evaluation of drug release profile from colloidal carriers-ultrafiltration technique at low pressure. *Int J Pharm*. 1993;94:115-123.

5. Muller RH, Ruhl D, Runge S, Schulze-Foster K, Mehnert W. Cytotoxicity of solid lipid nanoparticles as a function of the lipid matrix and the surfactant. *Pharm Res*. 1997;14:458-462.

6. zur Muhlen A, Schwarz C, Mehnert W. Solid lipid nanoparticles (SLN) for controlled drug delivery-Drug release and release mechanism. *Eur J Pharm Biopharm*. 1998;45:149-155.

7. Muller RH, Maassen S, Weyhers H, Mehnert W. Phagocytic uptake and cytotoxicity of solid lipid nanoparticles (SLN) sterically stabilized with Poloxamine 908 and Poloxamer 407. *J Drug Target*. 1996;4:161-170.

8. Schwarz C, Mehnert W. Solid lipid nanoparticles (SLN) for controlled drug delivery. II. Drug incorporation and physicochemical characterization. *J Microencapsul*. 1999;16:205-213.

9. Unruh T, Bunjes H, Westesen K, Koch MHJ. Investigations on the melting behaviour of triglyceride nanoparticles. *Colloid Polym Sci*. 2001;279:398-403.

10. Cavalli R, Caputo O, Carlotti ME, Trotta M, Scarnecchia C, Gasco MR. Sterilization and freeze-drying of drug-free and drug-loaded solid lipid nanoparticles. *Int J Pharm*. 1997;148:47-54.

11. Siekmann B, Westesen S. Thermoanalysis of the recrystallization process of melt-homogenized glyceride nanoparticles. *Colloids Surf B Biointerfaces*. 1994;3:159-175.

12. Westesen K, Bunjes H, Koch MHJ. Physicochemical characterization of lipid nanoparticles and evaluation of their drug loading capacity and sustained release potential. *J Control Release*. 1997;48:223-236.

13. Bunjes H, Drechsler M, Koch MHJ, Westesen K. Incorporation of the model drug Ubidecarenone into the solid lipid nanoparticles. *Pharm Res*. 2001;18:287-293.

14. Bunjes H, Koch MHJ, Westesen K. Effect of surfactants on the crystallization and polymorphism of lipid nanoparticles. *Prog Colloid Polym Sci*. 2002;121:7-10.

15. Bunjes H, Koch MHJ, Westesen K. Influence of emulsifiers on the crystallization of solid lipid nanoparticles. *J Pharm Sci*. 2003;92:1509-1520.

16. Bunjes H, Koch MHJ, Westesen K. Effect of particle size on colloidal solid triglycerides. *Langmuir*. 2000;16:5234-5241.

17. Mehnert W, Mader K. Solid lipid nanoparticles-production, characterization and applications. *Adv Drug Del Rev*. 2001;47:165-196.

18. Muller RH, Mader K, Gohla S. Solid lipid nanoparticles for controlled drug delivery-a review of the state of the art. *Eur J Pharm Biopharm*. 2000;50:161-177.

19. Yang S, Zhu J, Lu Y, Liang B, Yang C. Body distribution of camptothecin solid lipid nanoparticles after oral administration. *Pharm Res*. 1999;16:751-757.

20. Penkler L, Muller RH, Runge SA, Ravelli V. Pharmaceutical cyclosporine formulation with improved biopharmaceutical properties, improved physical quality and greater stability, and method for producing said formulation. WO 99/56733. 1999.

21. Zara GP, Cavalli R, Fundaro A, Bargoni A, Caputo O, Gasco MR. Pharmacokinetics of doxorubicin incorporated in solid lipid nanospheres (SLN). *Pharm Res*. 1999;40:281-286.

22. Jaeghere FD, Doelker E, Gurny R. Nanoparticles. In: Mathiowitz E, ed. *Encyclopedia of Controlled Drug Delivery*. Vol 2. New York, NY: John Wiley; 1999:641-664.

23. Woodle MC, Lasic DD. Sterically stabilized liposomes. *Biochim Biophys Acta*. 1992;1113:171-199.

24. Senior JH. Fate and behavior of liposomes in vivo: a review of controlling factors. *Crit Rev Ther Drug Carrier Syst*. 1987;3:123-193.

25. Arulsudar N, Subramanian N, Mishra P, Sharma RK, Murthy RSR. Preparation, characterization and biodistribution of ^{99m}Tc-labeled liposome encapsulated cyclosporine. *J Drug Target*. 2003;11:187-196.

26. Chamberlain M. Recurrent brainstem gliomas treated with oral VP-16. *Neuro-oncol*. 1993;15:133-139.

27. Ashley D, Meier L, Kerby T, et al. Response of recurrent medulloblastoma to low-dose oral etoposide. *J Clin Oncol*. 1996;14:1922-1927.

28. Subramanian N, Arulsudar N, Chuttani K, Mishra P, Sharma RK, Murthy RSR. Radiolabeling, biodistribution and tumor imaging of stealth liposomes containing methotrexate. *J Alasbimn*. 2003;6(22):Article 6.

29. Arulsudar N, Subramanian N, Mishra P, Chuttani K, Sharma RK, Murthy RSR. Preparation, characterization and biodistribution of Technetium-99m-labeled leuprolide acetate-loaded liposomes in Ehrlich Ascites tumor bearing mice. *AAPS PharmSci*. 2004;6:E5.

30. Richardson VJ, Jeyasingh K, Jewkes RF. Properties of [^{99m}Tc] technetium labeled liposomes in normal and tumor bearing rats. *Biochem Soc Trans*. 1977;5:290-291.

31. Theobald AE. Theory and practice. In: Sampson CB, ed. *Textbook of Radiopharmacy*. New York, NY: Gordon and Breach; 1990:127-129.

32. Mishra AK, Iznaga-Escobar N, Figueredo R, et al. Preparation and comparative evaluation of ^{99m}Tc-labeled 2-Iminothiolane modified antibodies and CITC-DTPA immunoconjugates of anti-EGF-receptor antibodies. *Methods Find Exp Clin Pharmacol*. 2002;24:653-660.

33. Siekmann B, Westesen K. Submicron-sized parenteral carrier systems based on solid lipids. *Pharm Pharmacol Lett*. 1992;1:123-126.

34. Westesen K, Siekmann B, Koch MHJ. Investigations on the physical state of lipid nanoparticles by synchrotron radiation X-ray diffraction. *Int J Pharm*. 1993;93:189-199.

35. Westesen K, Siekmann B. Investigations on the gel formation of phospholipids stabilized solid lipid nanoparticles. *Int J Pharm*. 1997;151:35-45.

36. Siekmann B, Westesen K. Melt-homogenized solid lipid nanoparticles stabilized by the nonionic surfactant tyloxapol. I. Preparation and particle size determination. *Pharm Pharmacol Lett*. 1994;3:194-197.

37. Aoki H, Sun C, Fuji K, Miyajima K. Disposition kinetics of liposomes modified with synthetic aminoglycolipids in rats. *Int J Pharm*. 1995;115:183-191.

38. Nabar SJ, Nadkarni GD. Effect of size and charge of liposomes on biodistribution of encapsulated ^{99m}Tc-DTPA in rats. *Ind J Pharmacol*. 1998;30:199-202.

39. Levchenko et al. Liposome clearance in mice: the effect of a separate and combined presence of surface charge and polymer coating. *Int J Pharm*. 2002;240:95-102.

40. Sengupta S, Tyagi P, Velpandian T, Gupta YK, Gupta SK. Etoposide encapsulated in positively charged liposomes: pharmacokinetic studies in mice and formulation stability studies. *Pharmacol Res*. 2000;42:459-464.

41. Yu HY, Lin CY. Uptake of charged liposomes by the rat liver. *J Formos Med Assoc*. 1997;96:409-413.

42. Hernandez-Caselles T, Villalain J, Gomez-Fernandez JC. Influence of liposome charge and composition on their interaction with human blood serum proteins. *Mol Cell Biochem*. 1993;120:119-126.

43. Duncan R. Polymer conjugates for tumor targeting and intracytoplasmic delivery. The EPR effect as a common gateway? *Pharm Sci Tech Today*. 1999;2:441-449.